Available online at www.elixirpublishers.com (Elixir International Journal)

Applied Chemistry

Elixir Appl. Chem. 63 (2013) 18659-18665

ISSN: 2229-712X

Dye Removal Using Some Surface Modified Silicate Minerals

K.A. Selim*, M.A. Youssef, F. H. Abd El –Rahiem and M.S. Hassan

Central Metallurgical Research and Development Institute (CMRDI) P.O. Box: 87 Helwan, Cairo, Egypt.

ARTICLE INFO

Article history:

Received: 27 August 2013;

Received in revised form:

2 October 2013;

Accepted: 21 October 2013;

Keywords

Glauconite,
Bentonite,
Dye removal,
Modified Silicate minerals,
Adsorption.

ABSTRACT

The objective of this work is to study the efficiency of some surface modified phyllosilicate minerals (bentonite and glauconite) in the removal of dyes from textile waste water. It is found that complete dye removal was achieved by using (10-25) g modified glauconite from solutions having a dye concentration of 10-50 mg/L. Adsorption data were modeled using Langmuir, Freundlich, Temkin and Dubinin-Radushkevich isotherms. Adsorption capacities and optimum adsorption isotherms were predicted by linear regression method. The analysis of experimental isotherms showed that Langmuir isotherm reasonably fit the experimental data in the studied concentration range for the adsorption of dye onto glauconite mineral surface where Freundlich isotherm fit the experimental data for the adsorption of dye onto bentonite mineral surface.

Introduction

The world-wide high level of production and use of dyes generates colored wastewaters, which give cause of environmental concern due to their impact on water bodies, and growing public concern due to their toxicity and carcinogenicity. Textile companies, dye manufacturing industries, paper and pulp mills, tanneries, electroplating factories, distilleries, food companies and a host of other industries discharge colored wastewater. As a matter of fact, the discharge of such effluents in the environment is worrying for both toxicological and esthetical reasons. The methods of color removal from industrial effluents include biological treatment, coagulation, floatation, adsorption, oxidation and hyper filtration. Among the treatment options, adsorption appears to have considerable potential for the removal of color from industrial effluents [1]. The process of adsorption has an edge over the other methods due to its sludge free clean operation and completely removed dyes, even from the diluted solution. The major advantage of an adsorption system for water pollution control are less investment in terms of both initial cost and land, simple design and easy operation, no effect by toxic substance, and superior for the removal of organic waste constituents as compared to the conventional biological treatment processes.

The physico-chemical properties of clay minerals are the basis for their technological applications. Such properties are closely linked to the mineral fabric, surface area, porosity, crystal morphology, structure and composition. These properties can vary with thermal and mechanical treatment [2-6]. The above mentioned treatments could lead to loss of water, modification of the surface characteristics, porosity and partial destruction of structure [7]. Also, these treatments could lead to enhancement of some technologically important properties as adsorption capacity, catalyst support, and absorbency [8].

In this paper, Different modification techniques have been tested to get the information on treating such effluents in this study. The composition and structure of the minerals were studied by X-Ray Diffraction (XRD) and Fourier Transform IR (FTIR) spectroscopy. In addition, Scanning Electron Microscope (SEM) and Energy Dispersive Spectroscope (EDS) were used for surface morphology observations and for evaluation of the modification efficiency.

Materials and Methods

Materials

The bentonite mineral was collected from Northern Coast of Egypt. About 85 % of the collected sample is a high iron montmorillonite with some substitutions of Al^{3+} for Si^{4+}. The principle exchangeable cation is calcium. The main associated gangues are kaolin and quartz. Meanwhile, glauconite mineral was collected from new valley locality, Egypt and it consists of spherical, loaf-like or ellipsoidal, grass green aggregates (pellets) of glauconite in addition to quartz. Methyl violet dye used in this study was supplied by Air Products and Chemicals, Inc.

Methods

Surface Modification of the Two Minerals

Ca-montmorillonite sample was calcined at different temperature (600-900ºC) for two hours. The calcined samples were treated with 25 wt. % sulfuric acid for one hour at 98ºC [9]. The activated samples were washed several times until the removal of aluminum sulfate. After that, the samples were dried overnight at 60ºC.

Glauconite sample was screened to the proper effective size (–850 + 250 µm), followed by water soaking, (1:3) solid/liquid ratio, and shacked gently from time to time. The turbidity of water was measured from time to time to confirm the removal of clay from the glauconite surface using a Turbidity Meter, HI 93703, Micro-processor, HANNA Instruments. The treatment was applied through a series of washing cycles.

Separation Experiments

The separation experiment was carried out in glass column, 25 mm diameter and 50 cm height which filled with 10-15 g (5-7.5 cm height) of treated minerals. The column was saturated with water then 200 ml of dye solution was added at the top of the column at a flow rate of 10 ml/min. The initial dye concentration ranged from 10 - 100 mg/L was studied. The concentration of dye in the filtrate was determined through

Tele:
E-mail addresses: k2selem1@gmail.com

measurement of total organic carbon content in the supernatant using a 'Phoenix 8000' Total Carbon Analyzer", TOC. The average of three readings was taken as a measure for dye concentration. All the experiments were done at room temperature (~ 25 ± 2 ^{o}C).

Characterization

A Philips PW 1730 powder X-ray diffractometer with Fe-filtered Co (K-alpha) run at 30 kV and 20 mA was used to examine Ca-montmorillonite and glauconite minerals. Infrared vibrational spectra were recorded on a Nicolet Magna 750 Fourier-transform spectrometer. For each sample, 28 scans were accumulated over the 4000-400 cm^{-1} spectral range employing the transmittance mode and a resolution of 4 cm^{-1}. The pressed KBr disc employed for this purpose was prepared using 0.4 mg of sample and 200 mg of KBr. Selected samples were observed on fractured surface under a JSM-6400 scanning electron microscope (SEM) to examine the morphology of montmorillonite and glauconite before and after treatment. A Laser particle size analyzer "FRITSCH" model "Analystte 22" was employed for size analysis of samples before and after treatment. Quantachrome NOVA 1200 was used for measurement of specific surface area and porosity.

Adsorption Equilibrium Study

Batch adsorption experiments were carried out at room temperature (25°C ± 2). Exactly 100 mL of reactive dye solution of known initial concentration, (*Ci*) (10–100 mg L^{-1}) was shaken at the constant agitation speed (200 rpm) with a required dose of adsorbents (10–25 g) for a specific period of contact time (5–180 min) in a mechanical shaker, after noting down the initial pH of the solution to the optimum pH. The pH of the solutions was adjusted by adding either 1M HCl or 1M NaOH solution. After equilibrium, the final concentration (*Ce*) were measured. The percentage removal of dye were calculated using the following relationship:

$$\%\ \boldsymbol{Removal\ of\ dye} = \frac{(Ci-Ce)}{Ci} \times 100 \quad \text{.....(1)}$$

where *C*i and *C*e are the initial and final (equilibrium) concentrations of dye (mg L^{-1}), respectively [10].

The adsorption capacity, q_e (mg/g), was calculated according to the following equation:

$$q_e = \frac{(C_o - C_e)V}{W} \quad \text{.....(2)}$$

Where C_o and C_e are the initial and equilibrium solution concentrations (ppm), respectively, V, the volume of the solution (L), W is the weight of the sample (bentonite and glauconite) in grams [11] .

Adsorption Isotherm Models

The equilibrium adsorption of methyl violet dye onto bentonite and glauconite minerals was analyzed using Langmuir, Freundlich, Temkin and Dubinin – Radushkevich isotherms.

Langmuir Isotherm

Langmuir model is the simplest theoretical model for monolayer adsorption onto a surface with finite number of identical sites, [12-14]. The general Langmuir equation is as follows:

$$q_e = \frac{k_L C_e}{1 + a_L C_e} \quad \text{.....(3)}$$

When linearized, Equation (2) becomes:

$$\frac{C_e}{q_e} = \frac{1}{k_L} + \frac{a_L C_e}{k_L} \quad \text{.....(4)}$$

k_L and a_L are the equilibrium constants. Plotting C_e/q_e against C_e yields a straight line with slope, a_L/K_L, and intercept $1/K_L$. The ratio a_L/K_L indicates the theoretical monolayer saturation capacity, Q_0.

Freundlich Isotherm

Freundlich expression is an empirical equation applicable to non-ideal sorption on heterogeneous surface as well as multilayer sorption. The model is given as

$$q_e = K_F C_e^{1/n} \quad \text{.....(5)}$$

Equation (5) is linearized into logarithmic form for data fitting and parameter evaluation as follows:

$$Log\ q_e = Log\ K_F + \frac{1}{n} Log\ C_e \quad \text{.....(6)}$$

By plotting Log q_e versus *Log*C_e, constant K_F and exponent *1/n* can be calculated.

Temkin Isotherm

The Temkin isotherm [15] has been used in the following form:

$$q_e = \frac{RT}{b} \ln(A C_e) \quad \text{.....(7)}$$

Using equation 7 to analyze the sorption data, a plot of q_e versus ln*Ce* enables determination of constants *A* and *b*.

Dubinin-Radushkevich Isotherm

This isotherm model was chosen to estimate the characteristic porosity of the biomass and the apparent energy of adsorption. The model is represented by the equation below:

$$q_e = q_D\, e^{(-B_D[RT\ln\left(1+\frac{1}{C_e}\right)]^2)} \quad \text{.....(8)}$$

Where, B_D is related to the free energy of sorption per mole of the sorbate as it migrates to the surface of the biomass from infinite distance in the solution and q_D is the Dubinin-Radushkevich isotherm constant related to the degree of sorbate sorption by the sorbent surface [16]. The linear form of equation (9) is given as:

$$ln\ q_e = ln\ q_D - 2B_D\ RT \ln\ (1 + \frac{1}{C_e}) \quad \text{.....(9)}$$

Results and Discussion

Minerals Composition

Fig.1, indicated that the Egyptian bentonitic clay was dominated by Ca-montmorillonite associated with traces of kaolinite and quartz. On the other hand, the XRD pattern of glauconitic material shows that it is composed of set of reflections, characteristic of the 1M-glauconite poly-type associated with quartz, Fig.2. and Table 1, show the chemical compositions of the two raw materials.

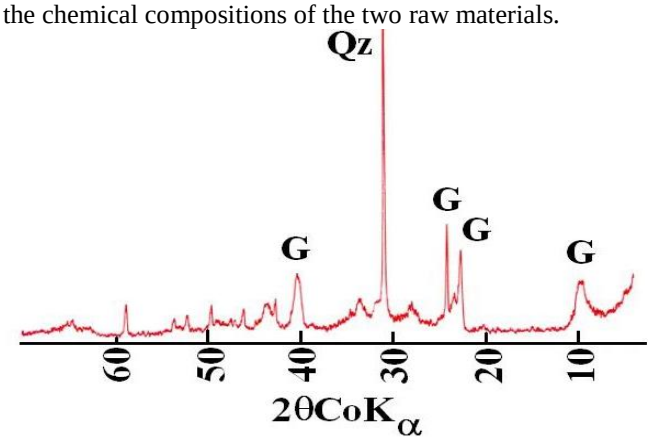

Fig.1. XRD pattern of bentonite

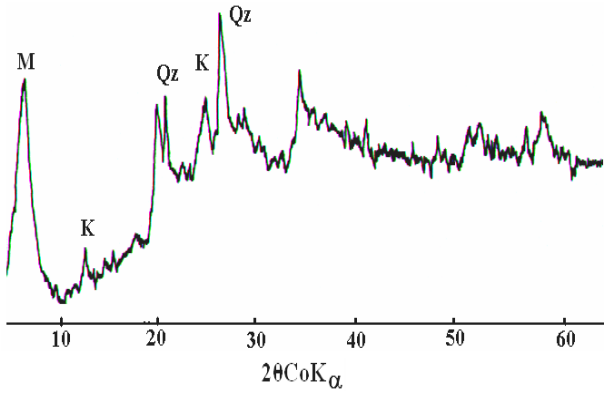

Fig.2. XRD of glauconitic material

Table 1: Chemical analysis of bentonite and glauconite minerals

Oxides	Bentonite	Glauconite
SiO_2	55.12	46.00
Al_2O_3	16.14	5.80
K_2O	1.05	7.29
CaO	1.17	2.40
Na_2O	1.41	Zero
TiO_2	1.18	0.11
P_2O_5	Zero	0.86
MnO	Zero	0.20
Fe_2O_3	8.25	22.85
MgO	2.86	3.23
L.O.I	12.35	10.95
Total	99.53	99.69

FTIR Analysis

The most prominent feature of the FTIR spectrum of the bentonite, Fig.3, is the presence of a wide band at 1027 cm^{-1} which is corresponding to the Si-O stretch of the phyllosilicate clay structure [17]. This band was not fully resolved because of the considerable thickness of the clay film. Bands at 3627 cm^{-1} and 3692 cm^{-1} are due to the stretching vibrations of structural OH groups, and the band at 3692 cm^{-1} is characteristic of kaolinite while the 3627 cm^{-1} band is commonly found in phyllosilicate minerals [18]. The band at 690 cm^{-1} corresponds to the structural vibration of the OH group, while the band at 919 cm^{-1} corresponds to the deformation mode of the Al_2OH group. The shoulder band at 880 cm^{-1} may be assigned to AlFeOH vibrations, thereby demonstrating the presence of iron in the octahedral sheets of montmorillonite [17]. The remaining bands were assigned to vibrations arising from water molecules as the bands at 3426 cm^{-1} which corresponds to the stretching vibrations (ν_3 and ν_1 modes), whereas the 1642 cm^{-1} band corresponds to H-O-H bending in the water molecule (ν_2 mode).

On heating Ca-montmorillonite up to 900°C, the broad band at 1027 cm^{-1} assigned to complex Si-O stretching vibrations in the tetrahedral sheet moved to 1046 cm^{-1}, Fig.3. Meanwhile, the treatment of calcined montmorillonite with H_2SO_4 increases the intensities of Si-O vibration bands of amorphous silica as shown at 1100 cm^{-1}, 800 cm^{-1} and 469 cm^{-1}. The FTIR spectrum of glauconite, Fig.4, is characterized by stretching vibration band of -OH at 3538 cm^{-1} and the deformation band at 801 cm^{-1}. The silicate network is characterized by stretching vibration bands at 1060 cm^{-1} for Si-O and 998 cm^{-1} for Si-O-Si and deformation band at 488 cm^{-1} for Si-O-Fe.

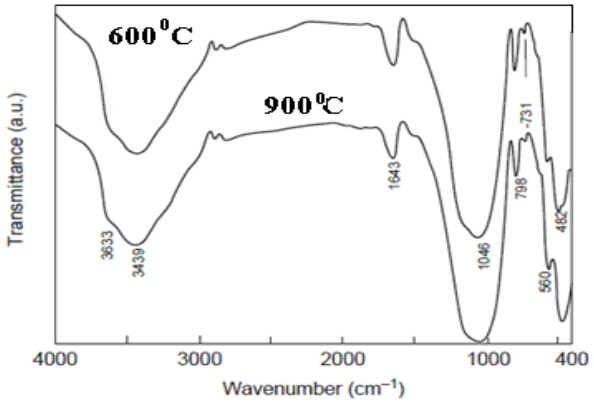

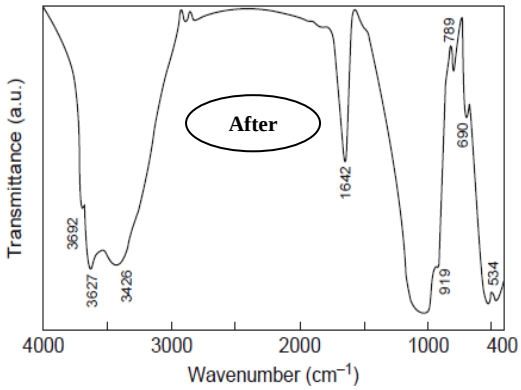

Fig.3. FTIR of bentonite before and after heat treatment

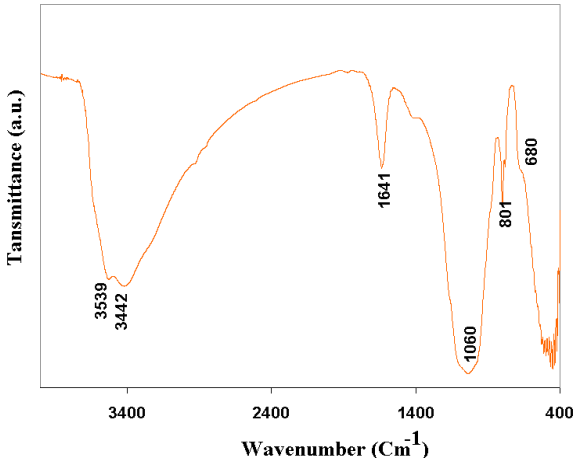

Fig.4. FTIR of glauconite

Morphological Studies

Figure 5a exhibits the typical morphology for calcium montmorillonite sample. As noticed, the mineral consists of complex aggregates of grains of few microns in size. The edges of these grains are sharp and rugged. The granular aggregates, as a rule, are not transparent to an electron beam. The tactoid morphology (face-to-face aggregation) of montmorillonite may be related to its moderate CEC value and the relative large particle size [19]. This morphology affects the surface area and porosity of this mineral. Heating the montmorillonite led to loosening of this morphology with the complex aggregates. The characteristic morphological features of the heated montmorillonite are thin and short leaves, onion-shaped, honeycomb, lath-shaped and dispersed thin flakes, Figs. 5b and 5c.

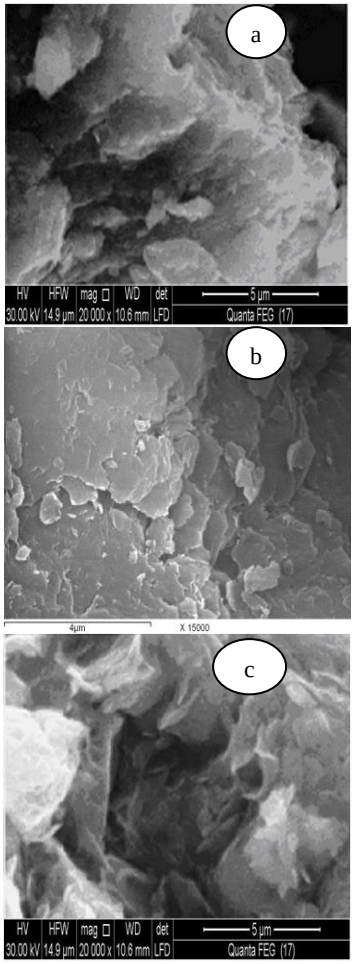

Fig.5. SEM images of Ca- montmorillonite (a), modified montmorillonite at 600ºC (b) and at 900ºC (c)

Fig. 6A, shows the typical morphology of untreated glauconite which has sphere-like shape. Small cavities and cracks are present on the surface of each glauconitic particle. This nature of rough texture provides good active sites for chemical adsorption. On the other hand, Fig. 6B shows the morphology of glauconite after treatment. As shown, there is a noticeable change in the morphology that can be represented by the appearance of large number of pores with different sizes. There is a noticeable increase for the total pore area, (29.38 m^2/g) to (38.99 m^2/g) due to the removal of clays and elements that occupy these pores, EDS Analysis, Fig. 7.

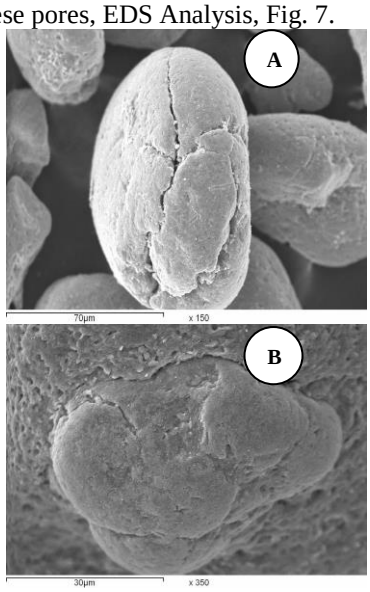

Fig.6. SEM images of glauconite; (A) Original (B) Washed

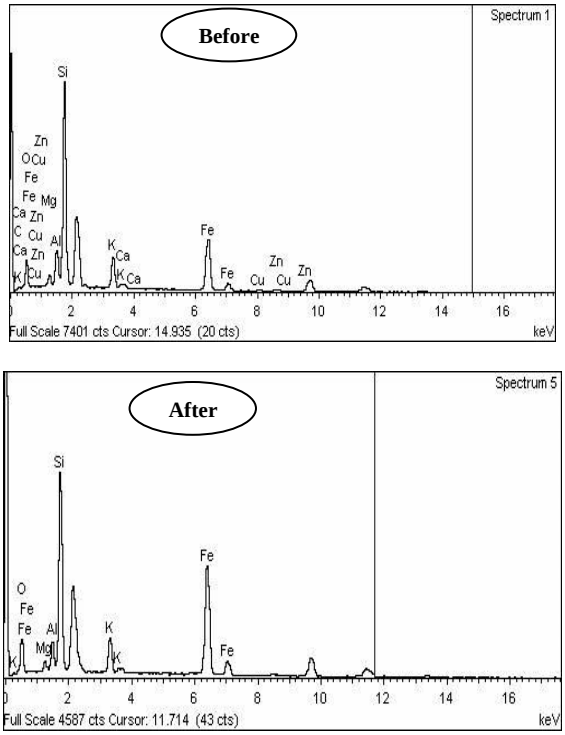

Fig.7. EDS Analysis spectrum of Glauconite before and after treatment

In general, clays have a large capacity for adsorbing organic compounds. Expanding 2:1 type layer silicates are especially reactive towards organic materials and uncharged polar molecules, because the ability of organic species to enter the interlayer space forming intercalation complexes. Large surface area, particle size distribution and pore volume play important roles in adsorption capacity of clay minerals. Calcination of the layered silicate resulted in the production of variations in the specific surface area and mean particle size as shown in Fig. 8 where surface area increased from 0.85 m^2/cc to 0.95 m^2/cc. At the same time, the mean particle size, d_{50}, decreased from 19.58 µm to15.25 µm. Calcination process caused variations in the mesopore volume, nature and number of Lewis and Bronsted surface sites, producing a colloidal gel [7].

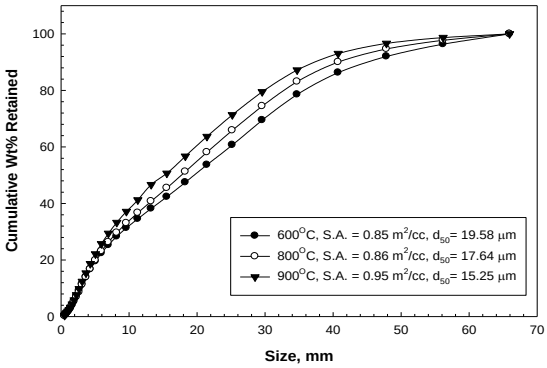

Fig.8. Size Distribution of bentonite from 600-900 °C

The increase in surface area and mesopores may be ascribed to the attack on some layers edges. This decomposition, which crumbles several layers in the edge region, creates a consideable amount of mesopores. The adsorption of dye by treated phyllosilicate minerals (glauconite and bentonite) reaches equilibrium conditions when the adsorbent stops adsorbing the solute dye. The adsorption equilibrium point is indicated through determination of concentration of dyes in the effluent.

At this point the concentration of the dye in the effluent becomes equal to the initial concentration.

The initial concentration of dyes is an important parameter and a main limiting factor, since a given mass of adsorbent can only adsorb a fixed mass of dye. The increase in the initial dye concentration at a constant flow rate increases the slope of breakthrough curve and decrease the throughput (output) until breakthrough. This may be caused by high initial concentration saturating the adsorbent more quickly, thereby decreasing the breakthrough time. In general, an increasing initial dye concentration increased the critical bed depth of adsorption column and increases the adsorption capacity.

The rate of adsorption decreased with increasing the initial concentration. The percentage removal and amount of dye adsorbed at different initial concentration of dye were tabulated in Table 2. Modified glauconite mineral showed better results than that of modified bentonite mineral which may be due to the excellent surface structure of modified glauconite. The maximum dye removal (100%) was achieved by using (10-25) g of modified glauconite for solution having a dye concentration of 10-50 mg/L, Fig.9. On the other hand, for modified bentonite, the maximum dye removal (70%) was achieved for a solution having a dye concentration of 10 mg/L. At a fixed breakthrough and defined/constant operating conditions, the critical bed height increased with increasing the initial dye concentration, which agrees well with the experimental results and also with the literature report [20].

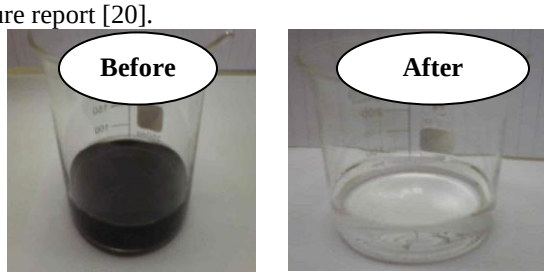

Fig.9. Dye before and after Removal

Adsorption Capacity

The adsorption of different concentrations of methyl violet dye onto both bentonite and glauconite mineral particles is shown in Fig. 10. The maximum adsorption capacities of the dye were 4 and 7 mg/g respectively. As mentioned before, the percentage removal of the dye was found to decrease with the increase of initial dye concentration. This indicates that there is a reduction in immediate solute adsorption, owing to the lack of available active sites required for the high initial concentration of methyl violet dye. At the same time, the rate of removal is higher at the beginning due to the larger surface area available for adsorption. After adsorption, the rate of dye uptake is controlled by the rate of dye transported from the exterior to the interior sites of the adsorbent particles [21].

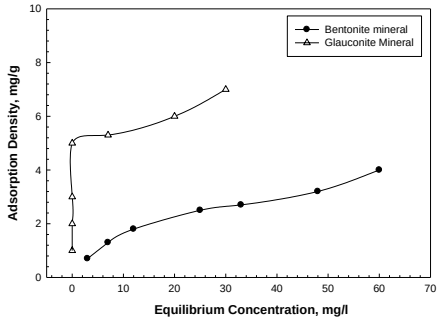

Fig.10. Adsorption Isotherm of Methyl Violet Dye onto Bentonite and Glauconite Minerals

Table 2: The amount of dye adsorbed by modified bentonite and glauconite minerals as a function of initial dye concentration.

Initial dye conc., ppm	Bentonite		Glauconite	
	Final dye conc., ppm	% Removal	Final dye conc., ppm	% Removal
10	3	70	Zero	100
20	7	65	Zero	100
30	12	60	Zero	100
50	25	50	Zero	100
60	33	45	7	88.33
80	48	40	20	75
100	60	40	30	70

Adsorption Isotherms

In order to optimize the design of an adsorption system to remove the dye, it is important to establish the most appropriate correlations for the equilibrium data for each system. Equilibrium studies that give the capacity of the adsorbent and the equilibrium relationships between adsorbent and adsorbate are described by adsorption isotherms which are usually the ratio between the quantity adsorbed and the remaining in solution at fixed temperature at equilibrium. Langmuir and Freundlich isotherms are the earliest and simplest known relationships describing the adsorption equation [21]. These two isotherms beside Temkin and Dubinin-Radushkevich isotherm models were used to access the different isotherms and their ability to correlate experimental data.

Langmuir Isotherm

As mentioned before, the Langmuir isotherm was chosen for the estimation of maximum adsorption capacity corresponding to complete monolayer coverage on both bentonite and glauconite surfaces. It is well known that the Langmuir equation is intended for the homogenous surface. The experimental data were fitted into equation (4) for linearization, for both bentonite and glauconite as shown in Fig.11 and Fig.12 respectively. The linear regression equations and determination coefficient (R^2) generated are shown in Table 3.

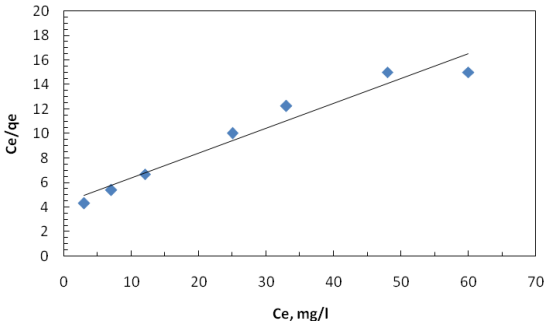

Fig. 11. Langmuir Plot for Bentonite

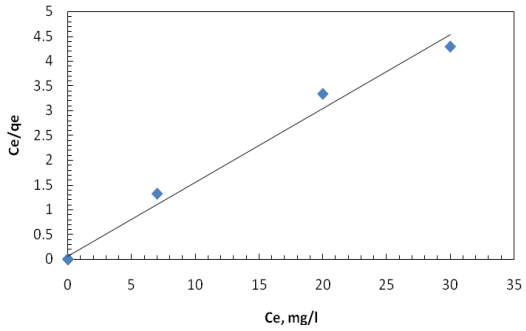

Fig. 12. Langmuir Plot for Glauconite

Table 3. Linear Regression Equations and Coefficients of Determination (R^2) for Different Isotherm Models

Bentonite /Dye	Glauconite/Dye
Langmuir Isotherm	
Y = 0.203 X + 4.342 R^2 = 0.954	Y = 0.148 X + 0.065 R^2 = 0.989
Freundlich Isotherm	
Y = 0.485 X - 0.287 R^2 = 0.986	Y = 0.176 X + 0.569 R^2 = 0.905
Temkin Isotherm	
Y = 1.013 X - 0.612 R^2 = 0.953	Y = 1.067 X + 3.130 R^2 = 0.881
Dubinin-Radushkevich Isotherm	
Y = -0.237 X + 1.218 R^2 = 0.929	Y = -0.094 X + 1.969 R^2 = 0.820

As noticed, the values of R^2 are 0.954 and 0.989 for bentonite and glauconite respectively. It means that Langmuir model gives a good fit to the adsorption process of methyl violet dye onto glauconite compared with bentonite as a confirmation of the chemisorptions process. These results were confirmed from values of Langmuir constants, a_L and K_L shown in Table 4.

Table 4. Different Isotherm Models' Constants for Dye Adsorption onto Bentonite and Glauconite minerals

Bentonite /Dye	Glauconite/Dye
Langmuir Isotherm	
a_L = 0.047 K_L = 0.2303	a_L = 2.277 K_L = 15.385
Freundlich Isotherm	
K_f = 0.516 n_f = 2.016	K_f = 3.71 n_f = 5.681
Temkin Isotherm	
b = 24.42 A_T = 0.547	b = 23.18 A_T = 18.79
Dubinin-Radushkevich Isotherm	
B_D = 0.1185 q_D = 3.380 E = 2.053	B_D = 0.047 q_D = 7.16 E = 3.23

Freundlich Isotherm

Freundlich isotherm model was chosen to estimate the adsorption intensity of methyl violet dye towards bentonite and glauconite mineral. It is an empirical equation employed to describe the isotherm data. Application of isotherm equation to analyze the equilibrium isotherms of bentonite and glauconite gave linear plots, Fig. 13 and Fig. 14.

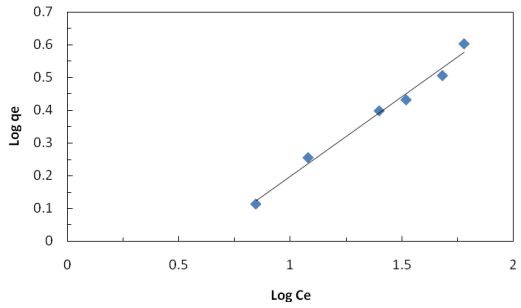

Fig. 13. Freundlich Plot for Bentonite

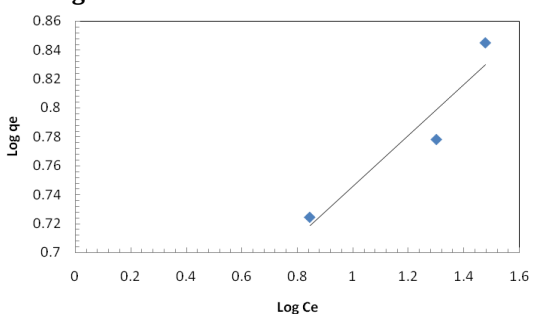

Fig. 14. Freundlich Plot for Glauconite

The linear regression equations and the regression coefficients (R^2) are shown in Table 3. The values of K_f and n_f, Table 4, determine the steepness and curvature of the isotherm [11]. The Freundlich equation gives an adequate description of adsorption data over a restricted concentration; also, it is suitable for a highly heterogeneous surface and an adsorption isotherm lacking a plateau including a multi-layer adsorption. The values of 1/n less than the unity for both bentonite and glauconite which is an indication that significant adsorption takes place at low concentration but the increase in the amount adsorbed with concentration becomes less significant at higher concentration [22]. The values of K_f confirm that the adsorption capacity of glauconite is higher than that in case of bentonite as the higher the K_f value, the greater the adsorption intensity.

Temkin Isotherm

From the results obtained, we can see that Temkin equation did not represent a bitter fit to the experimental data. The values of (R^2) are 0.881 and 0.953 for glauconite and bentonite respectively as shown in Table 3, Fig. 15 and Fig.16 indicating the poor adsorption of the methyl violet dye onto bentonite and glauconite surfaces.

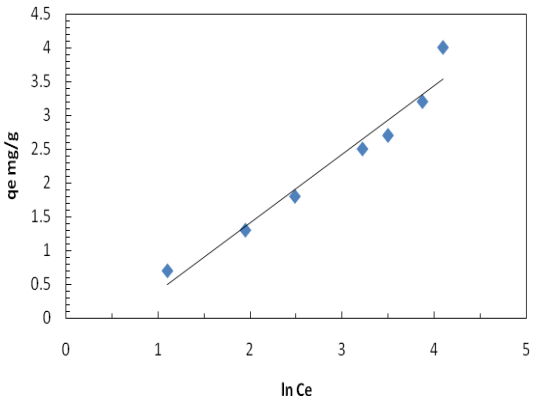

Fig. 15. Temkin Plot for Bentonite

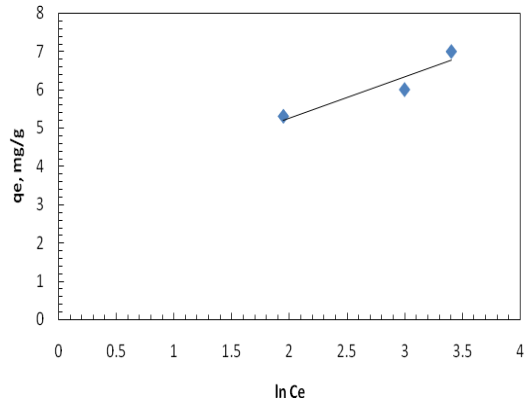

Fig. 16. Temkin Plot for Glauconite

Dubinin-Radushkevich Isotherm

Fig. 17 and Fig.18 represent the Dubinin-Radushkevich plots for the adsorption of methyl violet dye onto bentonite and glauconite. (R^2) values and constants for the model are given in Table 3 and Table 4. It is observed that Dubinin-Radushkevich isotherm did not give a good description for the adsorption process. The values of q_D are not high enough to indicate the adsorption capacity while the values of the apparent energy of adsorption, E, depict the physical adsorption process. Therefore D-R isotherm did not give a good fit to the adsorption process.

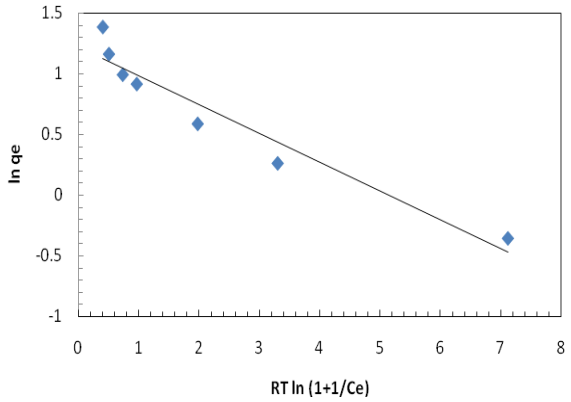

Fig. 17. Dubinin-Radushkevich Plot for Bentonite

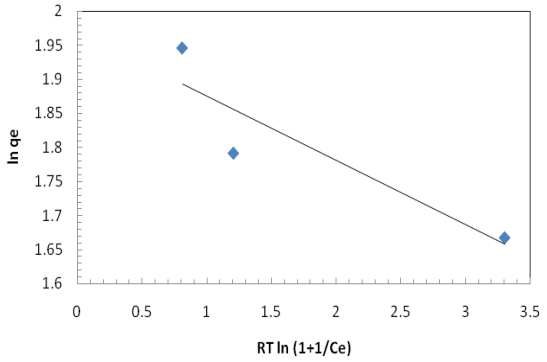

Fig. 18. Dubinin-Radushkevich Plot for Glauconite

Conclusions

The following major conclusions can be summarized based on this study:

1. Thermal treatment followed by acid activation was used to modify bentonite while glauconite was treated through a series of washing cycles.
2. Heating the montmorillonite led to loosening of the morphology, which caused variations in mesopore volume, nature and number of Lewis and Bronsted surface sites, producing a colloidal gel.
3. The rate of adsorption decreases with increasing in initial concentration.
4. The maximum dye removal was 100% and 70% for modified glauconite and modified bentonite, respectively.
5. The study on the equilibrium adsorption isotherms provides greater insights on the adsorption of methyl violet dye onto bentonite and glauconite surfaces.
6. The data obtained are best fitted only to Langmuir and Freundlich isotherms.
7. (R^2) values indicated that Langmuir isotherm is the best followed by Freundlich isotherm.

References

[1] N. K. Amin, Removal of reactive dye from aqueous solutions by adsorption onto activated carbons prepared from sugarcane bagasse pith, Desalination, 223 (2008) 152-161.

[2] Y. Shaobin Wang, A. Boyjoo, Choueib and Z.H. Zhu, Removal of dyes from aqueous solution using fly ash and red mud. Water Res., 39: (2005) 129- 138.

[3] S. Saiful Azhar, A. Ghaniey Liew, D. Suhardy, K. Farizul Hafiz and M.D. Irfan Hatim, Dye removal from aq. Soln., American Journal of Applied Sciences 2 (11) (2005) 1499-1503.

[4] K.N Nagarethinam. and M. Soundrapandian., Column studies on removal of dyes, EJEAFChe, 6 (3) (2007) 1860-1868.

[5] K. Okiel, M. El-Sayed and M. El-Kady, Treatment of bentonite and deposited carbon, Egyptian Journal of Petroleum 20, (2011) 9–15.

[6] E. Bojemueller, A. Nennemann and G. Lagaly, Enhanced pesticide adsorption by thermally modified Bentonites, Appl.Clay Sci., 18 (2001) 227-284.

[7] M. Hassan and H. El-Shall, Glauconitic clay of El Gidida, Egypt: evaluation and surface modification, Appl. Clay. Sci., 27 (2004) 219-222.

[8] G. Lagaly, surface and interlayer reactions: bentonite as adsorbents. Presented at 10th inter clay conf., Adelaide, Australia, 18-23 July (1995).

[9] A. Tabak, B. Afsin, B. Caglar and E. Koksal, Characterization of Turkish bentonite, Journal of Colloid and Interface Science, 313 (1) (2007) 5-11.

[10] G. McKay, J.F. Porter and G.R. Prasad, The removal of dye colours from aqueous solutions by adsorption on low-cost materials, Water, Air Soil Pollut., 114 (1998) 423–438.

[11] K.A. Selim and N. A. Abdel-Khalek, Comparative Evaluation of Adsorption Isotherms of Calcium Carbonate Coating by Polyacrylic Acid, The Journal of Ore Dressing, Vo.12 Issue 24 (2010) 35-41.

[12] Bajpai, A. K., Rajpoot, M., and Mishra, D. D., "Static and Kinetic Studies on the Adsorption Behavior of Sulfadiazene," *Adsorption*, 6 (2000) 349–357.

[13] Agyei,N. M., , Strydom, C. A., and Potgieter, J. H., "An Investigation of Phosphate Ion Adsorption from Aqueous Solution by Fly Ash and Slag," *Cem. Concr. Res.*, 30 (2000) 823–826.

[14] Abdullah, M.A., Chiang, L., and Nadeem, M.," Comparative evaluation of adsorption kinetics and isotherms of a natural product removal by Amberlite polymeric adsorbents" Chemical Engineering Journal 146 (2009) 370–376.

[15] Bhargava, D.S. and Sheldarkar, S. B., "Use of TNSAC in Phosphate Adsorption Studies and Relationships. Isotherm Relationships and Utility in the Field," *Wat. Res*., 27(2) (1993) 325–335.

[16] Jnr. Horsfall, M., Spiff, A. I., and Abia, A.A. Studies on the influence of mercaptoacetic acid (MAA) modification of cassava (*manihot sculenta cranz*) wastebiomass on the adsorption of Cu^{2+} and Cd^{2+} from aqueous solution. *Bulletin of the Korean Chemical Society*, July 2004, vol. 25, no. 7, p. 969-976.

[17] V. C. Farmer, The infrared spectra of minerals. Mineralogical Soc., London,(1974) 331-363.

[18] J. Madejova, M. Janek, P. Komadel, H.J. Herbert and H.C. Moog, FTIR analyses of bentonite from high salinary systems. Appl. Clay Sci. 20 (2002) 255–271.

[19] G.W. Brindley and G. Brown, (ed.) Crystal structure of clay minerals and their x-ray identification. Mineralogical Society, London, (1980) 197–248.

[20] L. Markovska, V. Meshko, and V. Noveski, Korean J. Chem. Eng. 18(2), (2001) 190-195.

[21] K.A. Selim, F. H. Abd El-Raheim and A. A. El-Midany, Kinetic Modeling and Equilibrium of Amphoteric Collector Adsorption on Silica and Hematite, TENSIDE. SURF. Dt., 46 (2009) 2.

[22] Teng, Hsisheng and Hsieh, Chien-To., Influence of surface characteristics on liquid-phase adsorption of phenol by activated carbons prepared from bituminous coal. *Industrial and Engineering Chemistry Research*, vol. 37, no. 9, (September 1998) p. 3618-3624.